

Correlated patterns of tracheal compression and convective gas exchange in a carabid beetle

John J. Socha^{1,*}, Wah-Keat Lee¹, Jon F. Harrison², James S. Waters³, Kamel Fezzaa¹ and Mark W. Westneat³

¹Advanced Photon Source, Argonne National Laboratory, Argonne, IL 60439, USA, ²Section of Organismal, Integrative and Systems Biology, Arizona State University, Tempe, AZ 85287, USA and ³Department of Zoology, Field Museum of Natural History, Chicago, IL 60605, USA

*Author for correspondence at present address: Department of Engineering Science and Mechanics, Virginia Tech, Blacksburg, VA 24061, USA (e-mail: jjsocha@vt.edu)

Accepted 3 September 2008

SUMMARY

Rhythmic tracheal compression is a prominent feature of internal dynamics in multiple orders of insects. During compression parts of the tracheal system collapse, effecting a large change in volume, but the ultimate physiological significance of this phenomenon in gas exchange has not been determined. Possible functions of this mechanism include to convectively transport air within or out of the body, to increase the local pressure within the tracheae, or some combination thereof. To determine whether tracheal compressions are associated with excurrent gas exchange in the ground beetle *Pterostichus stygicus*, we used flow-through respirometry and synchrotron x-ray phase-contrast imaging to simultaneously record CO₂ emission and observe morphological changes in the major tracheae. Each observed tracheal compression (which occurred at a mean frequency and duration of 15.6±4.2 min⁻¹ and 2.5±0.8 s, respectively) was associated with a local peak in CO₂ emission, with the start of each compression occurring simultaneously with the start of the rise in CO₂ emission. No such pulses were observed during inter-compression periods. Most pulses occurred on top of an existing level of CO₂ release, indicating that at least one spiracle was open when compression began. This evidence demonstrates that tracheal compressions convectively pushed air out of the body with each stroke. The volume of CO₂ emitted per pulse was 14±4 nl, representing approximately 20% of the average CO₂ emission volume during x-ray irradiation, and 13% prior to it. CO₂ pulses with similar volume, duration and frequency were observed both prior to and after x-ray beam exposure, indicating that rhythmic tracheal compression was not a response to x-ray irradiation *per se*. This study suggests that intra-tracheal and trans-spiracular convection of air driven by active tracheal compression may be a major component of ventilation for many insects.

Supplementary material available online at <http://jeb.biologists.org/cgi/content/full/211/21/3409/DC1>

Key words: beetle, convection, gas exchange, imaging, synchrotron x-ray, tracheal compression.

INTRODUCTION

Insects exchange respiratory gases through a complex network of tracheal tubes that open to the environment *via* spiracular valves. Although some insects are thought to transport gases through the tracheal system using diffusion alone (Krogh, 1920a; Weis-Fogh, 1964), many species are known to augment gas exchange using convection (Buck, 1962; Miller, 1966a). Two general mechanisms are recognized that produce convection in insect tracheal systems: (i) suction ventilation, in which air movement is driven passively by pressure differences (e.g. Miller, 1974), and (ii) collapse of tracheal tubes or air sacs, in which air is driven mechanically by active external or internal body movements that deform the tracheal system (e.g. Sláma, 1988). Until recently, internal processes in most insect species have been difficult to observe in live specimens, and previous understanding of convection by tracheal collapse has been based primarily on secondary inference. The historical inability to visualize tracheal structures has meant that mechanisms of active ventilation have not been thoroughly investigated in insects, and their role in gas exchange may be grossly underestimated. The relative importance of convection and diffusion in insect gas exchange thus remains an open question among the great diversity of insect taxa.

Convection in the tracheal system of insects has been recognized for over a century (see Babak, 1921). In suction ventilation, air is driven passively through the tracheae due to a pressure gradient between the tube interior and the external environment. Two variants are recognized. In Bernoulli suction ventilation, air is drawn into the main thoracic tracheae by pressure differences between the open ends of the tracheal system (Stride, 1958); this may occur in flying insects in which one spiracle is located in the fast-moving airstream and another is shielded from flow. This mechanism has only been identified in one species, the beetle *Petrognatha gigas* (Amos and Miller, 1966), but it is thought to occur in other species as well (Dudley, 2000). In passive suction ventilation, the pressure gradient is created by the depletion of tracheal oxygen when all spiracles are closed, lowering the intra-tracheal pressure; when the spiracles open, air flows in (e.g. Kestler, 1985; Mand et al., 2005; Miller, 1974; Schneiderman, 1960).

Most convection, however, is assumed to be produced *via* muscular contractions that deform tracheae or air sacs (Chapman, 1998). In this mechanism, muscles compress the exoskeleton, leading to a volume reduction of a tracheal tube or air sac, displacing air and forcing bulk flow. Depending on physical conditions (e.g. tube length and diameter, pressure differences, etc.), the resulting

convection can transport gases much faster than diffusion alone. Muscular convection behaviors include: (1) abdominal or thoracic pumping, in which a body segment is actively shortened in one dimension, causing an increase in hemolymph pressure (e.g. Harrison, 1997; Miller, 1971); (2) autoventilation, a form of thoracic pumping caused by the movement of the wings or legs during movement (e.g. Bartholomew and Barnhart, 1984; Weis-Fogh, 1967); and (3) hemolymph transport, in which hemolymph is pumped from one region of the body to another by the heart, locally increasing or decreasing pressure in different body compartments (e.g. Wasserthal, 1996). However, due to the previous inability to see through the opaque insect exoskeleton, deformation or movement of tracheal structures has been inferred rather than observed directly (but see Herford, 1938; Westneat et al., 2003) and, overall, the paradigmatic view of insect tracheal systems is that most tracheal tubes function as rigid, static conduits. Owing to this prior methodological limitation, for most insect taxa it is not known whether and which tracheal tubes collapse, under what conditions, and what functional roles the process serves. Convection in insect tracheal systems is thus poorly understood in terms of function, anatomical mechanism, and ecological and evolutionary significance.

Synchrotron x-ray imaging is a technique that has recently opened a new window to visualizing internal processes in small animals. Providing micrometer-scale resolution of millimeter-sized subjects, it enables an experimenter to view real-time events in living animals (Socha et al., 2007). More commonly used as a tool by physical science communities (Fitzgerald, 2000; Nugent et al., 2001), it has been applied only recently to questions of organismal biology (Westneat et al., 2008). Tracheal structures are particularly easy to visualize because of the large density difference between air and tissue, enabling for the first time direct observation of the morphology and dynamics of compressible tracheae in insects with opaque exoskeletons.

Convective mechanisms involving deformable tracheae have been studied recently using this form of x-ray imaging. By exploring a range of insect taxa, Westneat and colleagues (Westneat et al., 2003) discovered rapid cycles of collapse and reinflation in tracheal tubes of multiple species including a beetle (*Platynus decentis*), an ant (*Camponotus pennsylvanicus*) and a cricket (*Achaeta domestica*). The kinematics of these rhythmic tracheal compression cycles, which were observed in parts of the basal head and thorax, consisted of tube width decreasing dramatically in one axis while slightly increasing in the orthogonal axis, decreasing the volume by an estimated 50% on average. Compressions lasted for 0.7 to 1.6 s and occurred at a frequency of 24–42 cycles min^{-1} . The cycles were observed to occur synchronously in different tracheal tubes, but isolated compressions were noted in some species.

Although the volume displacement and rhythmicity of these newly discovered tracheal compression cycles strongly suggest a role in gas exchange, their specific biological function remains uncertain. One possibility is that tracheal compressions occur while spiracles are closed, driving pressure differences that enhance diffusion. Another possibility is that the compressions primarily drive airflow within the insect, between spiracles and tissues. Finally, tracheal compressions may flush the entire system, including producing convection through the spiracles (if synchronized with spiracular opening).

In this study, we focus on the function of tracheal collapse in a carabid beetle species (*Pterostichus stygicus*) that prominently compresses its tracheal tubes in a rhythmic fashion, specifically addressing the question of whether tracheal compressions produce

convection that increases gas exchange through the spiracles. To determine the connection between internal dynamics and external gas exchange, we imaged live beetles with synchrotron x-rays while simultaneously recording gas exchange patterns. Although many natural behaviors such as breathing and feeding are performed by insects in the synchrotron x-ray beam, this method can lead to a number of deleterious effects (including eventual death), depending on the location, energy, intensity and duration of exposure (Socha et al., 2007). Therefore, an important technical issue is whether the tracheal compressions observed with synchrotron imaging vanish or change their characteristics in undisturbed insects not being x-rayed. To control for this possible complication, we compared high-resolution CO_2 emission patterns before, during and after x-ray exposure.

MATERIALS AND METHODS

Animals

We studied the ground beetle *Pterostichus stygicus* Say (Coleoptera: Carabidae). Although previous work (Westneat et al., 2003) identified rhythmic tracheal compressions in the ground beetle *Platynus decentis*, we chose to work with *Pterostichus stygicus* for its larger body size (ca. 4–6 \times in mass), providing CO_2 signals of greater magnitude and tracheal tubes of larger maximum size for easier visualization. Preliminary exploratory x-ray imaging identified that *Pterostichus stygicus* compresses its tracheal tubes in a similar manner to *Platynus decentis*. Beetles were collected locally in pitfall traps in the woods at Argonne National Laboratory and were kept in a terrarium with *ad libitum* food and water prior to testing. Fifteen specimens (both male and female) were used, with mass 186.1 ± 44.3 mg (mean \pm s.d., hereafter).

Concurrent respirometry and x-ray imaging

To determine the relationship between gas exchange and internal compression of tracheal tubes, beetles were concurrently imaged with synchrotron x-rays while CO_2 release patterns were recorded (Fig. 1).

We used a positive pressure flow-through system to record CO_2 emission. Dry, CO_2 -free compressed air was flowed over the beetle in a respiratory chamber and subsequently measured with a carbon dioxide analyzer (LI-7000, LI-COR, Lincoln, NE, USA). Flow rate was maintained with a mass flow control valve (Sierra Instruments, Monterey, CA, USA) located prior to the chamber and connected to a mass flow controller [MFC-2, Sable Systems International (SSI), Las Vegas, NV, USA]. The length of tubing connecting the respiratory chamber to the carbon dioxide analyzer was 1.53 m. Data were transferred to a PC using an A/D converter (UI-2, SSI) and serial cable, and recorded at a sampling rate of 3.33 or 6.67 Hz using Expedata software (SSI).

Beetles were held immobile in a custom-made acrylic Plexiglas respirometry chamber. Two walls of the chamber were constructed of x-ray translucent polyimide film (Kapton, Dupont, DE, USA) so that the x-ray beam would pass through the sample unobstructed. The dimensions of the inner rectangular chamber containing the beetle were 0.5 cm \times 1.0 cm \times 2.0 cm, with a volume of 1.0 ml. Clay-like adhesive (Bostik Prestik, Bostik, Wauwatosa, WI, USA) was molded to the sides of the chamber to reduce the airflow volume, minimize washout time, and to keep the beetle immobile. With the beetle and clay in place, the remaining volume of air in the chamber was less than 0.25 ml.

Control trials were conducted to test whether the Prestik adhesive absorbed CO_2 . Boluses of air containing 301 p.p.m. CO_2 were injected into a 60 ml chamber with either a 5.5 g mass of

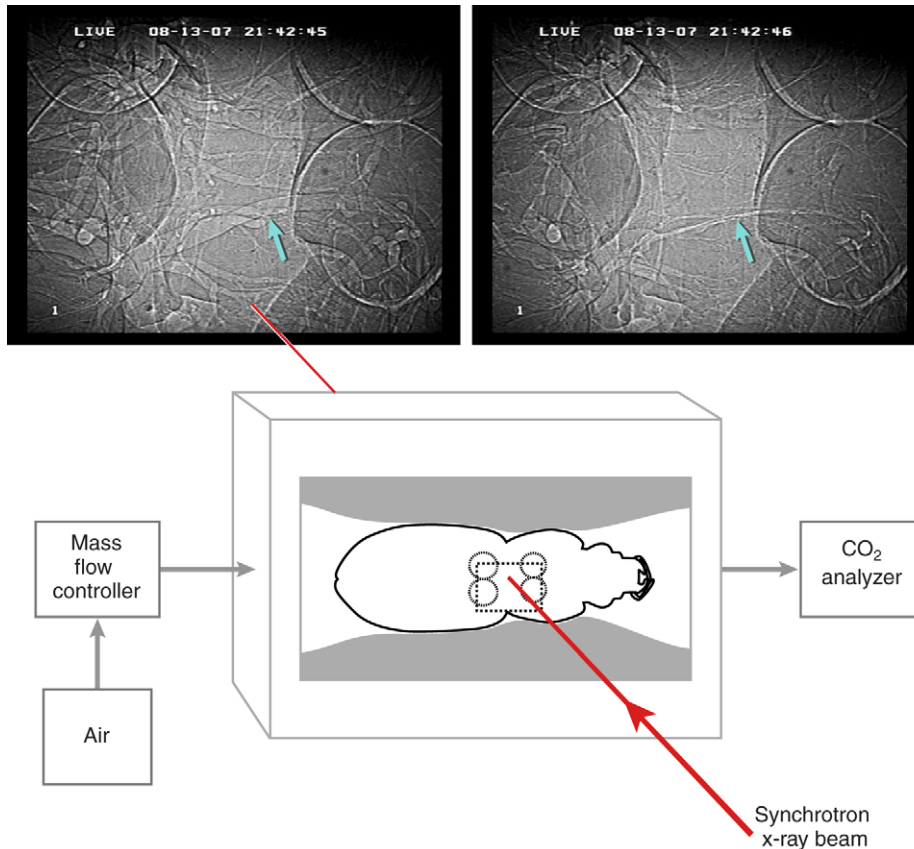


Fig. 1. Experimental setup used to simultaneously record CO₂ emission and visualize internal tracheal compression of the carabid beetle *Pterostichus stygicus*. Multiple locations in the body were recorded; x-ray movie stills here show tracheal tubes in the mesothorax between first and second coxae (large circular cuticular joints). The blue arrow indicates the location where we digitized the primary tube depicted in Fig. 3. Field of view is 3.2 mm × 2.4 mm. In the schematic diagram, legs are not depicted for clarity, but were tucked to the side of the beetle.

Prestik or a glass stopper (as control). The Prestik mass was shaped to match the size and volume of the stopper in order to create equivalent volumes and flow patterns within the chamber. The resulting CO₂ records show that boluses did not differ in volume (Student's *t*-test, d.f.=21, *t*=0.43), and that the chamber washout was similar for the two (*Z*-correction, 0.04 and 0.05, respectively), confirming that the Prestik adhesive did not significantly absorb CO₂.

The ground beetle *Platynus decentis* produces tracheal compressions with duration of the order of 1 s (Westneat et al., 2003). We used high flow rates (1.5–2.5 l min⁻¹), which, coupled with our small chamber volume, provided temporal resolution sufficient to identify similar potential CO₂ pulses in *Pterostichus stygicus*. High flow rates are required to prevent CO₂ pulses of short duration from being masked by washout in the respiratory chamber and tubing, and by transit through the infrared gas analyzer's detection chamber (Bartholomew et al., 1981; Gray and Bradley, 2006). In our system, the time constant (volume/flow rate) of the chamber was approximately 0.01 s, giving a 99% washout time of 0.05 s, and the transit time through the infrared gas analyzer's cylindrical detection chamber (length=152 mm, radius=4.8 mm) was 0.43 s. These parameters were sufficient to identify CO₂ events with sub-second precision. Although high flow rates mean that airspeed over the beetle was fast (~3 ms⁻¹, estimated), the spiracles of *Pterostichus stygicus* are shielded under the elytra or the thoracic ventral plates, so it is unlikely that significant flow-induced Bernoulli effects occurred in the tracheal system.

An additional factor to consider in designing a high-precision respiratory system is the transit time from chamber to CO₂ detector, which creates a time lag between gas release and its recording. Here this lag is critical to understanding the relative timing of gas

exchange and behaviors recorded with x-ray video. Theoretically, time lag can be calculated as:

$$\text{Time lag} = \frac{AL}{Q}, \quad (1)$$

where *A* is the cross-sectional area of the tubing, *L* is the length of tubing from chamber to detector, and *Q* is the gas flow rate. Given a 1/8 in (~0.32 cm) diameter tube of length 1.53 m and flow rate of 1.51 min⁻¹, the theoretical time lag in our system is 0.49 s. However, the time lag in practice is greater than predicted due to factors such as the uneven flow around the specimen, the presence of a particulate filter just upstream of the detector and diffusive spread of CO₂ during transit. To determine experimental values of time lag in our system, off-line trials were conducted using controlled CO₂ injections of known timing. A pressure-controlled picoliter volume ejector (Picospritzer III, Parker Hannifin Corporation, Fairfield, NJ, USA), which sends a 5 V signal at the time of injection, was used to measure the time lag directly. These trials were set up to simulate CO₂ release from the beetle in the respiratory chamber: CO₂ from the Picospritzer III was injected just upstream of the chamber, which contained a dead, dried beetle, and all else was the same. Time lag was measured as the time between the start of the voltage signal and the start of the detected CO₂ pulse (with start defined as the data point just prior to the first detectable rise in CO₂ in the pulse). The transit time of the CO₂ pulse from the Picospritzer to the free-stream flow was determined by varying the length of tubing from injection to the CO₂ detector and calculating the *y*-intercept of a linear regression of tube length vs lag time. This transit time (~0.26 s) was subtracted from the total measured time to provide the lag time. With a flow

rate of 1.51 min^{-1} , the experimentally determined lag time in our system was 0.90 s.

Synchrotron x-ray imaging

Synchrotron x-ray image data were collected at the XOR-IID and XOR-32ID undulator beamlines at the Advanced Photon Source (Argonne National Laboratory, Argonne, IL, USA). Phase-enhanced images were created using monochromatic x-rays (25 keV), a scintillator screen (cerium-doped yttrium aluminum garnet), and a sample-to-scintillator distance of $\sim 0.5 \text{ m}$. For more details of this method, see Socha et al. (Socha et al., 2007). To minimize potential harm to the animal, the lowest possible incident beam flux to form a viewable image was used; in some trials, shutters were used to reduce the field of view to the tracheal tube of interest, further reducing x-ray flux. Total exposure time on the animal was generally less than 15 min, and no apparent behavioral changes were observed in any specimen post-irradiation.

Images were recorded at standard video rates (30 Hz) using a video camera (Cohu 4920 or Cohu 2700, Cohu, San Diego, CA, USA) and a $\times 2$ microscope objective. The full field of view was $3.2 \text{ mm} \times 2.4 \text{ mm}$, and the reduced field of view (to reduce radiation exposure) was $3.2 \text{ mm} \times 1.3 \text{ mm}$. Movie clips were downloaded to a Macintosh computer using Adobe Premiere software (Adobe, San Jose, CA, USA).

Trial protocol

Beetles were anesthetized with N_2 , weighed to the nearest 0.1 mg with a Mettler AG245 balance (Mettler-Toledo, Columbus, OH, USA), and placed in the respiratory chamber, which was then mounted on a translatable stage in line with the x-ray beam. After the beetle had fully recovered from anesthesia (*ca.* 10 min), the chamber was connected to the flow-through respirometry system and the beetle's CO_2 release pattern was recorded for 5 min or longer. This pre-beam measurement provided a control against which we could compare respiratory patterns during x-ray exposure. The x-ray beam was then turned on, and the beetle was translated until a major tracheal tube of the mesothorax was brought into view. After 5 min of x-ray video recording showing rhythmic tracheal compression, the beetle was translated to view other parts of the body to determine the regions and tracheal tubes in which compression took place, and to determine whether such compressions occurred with the same timing as the compressions in the mesothorax. After the beam was turned off, the CO_2 recording was continued for 5 min or longer. Before and after each trial, air flow was diverted past the chamber to produce CO_2 -free baselines. Although the chamber was bypassed, prior testing was conducted to ensure that the empty chamber did not significantly alter the baseline. All trials were recorded at 21°C .

In each trial, a synchronization event was introduced both pre- and post-x-ray recording, which permitted the video and CO_2 signals to be synchronized *post hoc*. Two methods were used. In early trials, a mark in the CO_2 trace was made using a keyboard stroke concurrent with the time of beam on and beam off, providing synchrony of $\pm 0.97 \text{ s}$. This level of synchrony enabled us to associate pulses in the CO_2 trace with compressions observed in the movies. To obtain greater precision of timing of events, in later trials we synchronized the signals using pulses of light instead of keyboard strokes. The light was produced using a voltage source connected to the UI-2, with a voltage spike recorded in Expedata at the same time that the light pulse was recorded on videotape. This method provided synchronization of $\pm 0.07 \text{ s}$.

Analyses

Fifteen trials were recorded (one per specimen), and 10 were selected for detailed analysis. For each trial, the x-ray video was analyzed frame by frame to determine the kinematics of tracheal compression. In the mesothorax, the beginning and end of each tracheal compression were noted in a subsample of 2 min. These data were used to calculate compression duration and frequency, and were mapped onto the CO_2 trace to characterize the relationship between compression and gas release. Similar analyses were conducted in different regions of the body in representative trials.

The kinematics of compression in deformable tracheal tubes were broadly characterized by digitizing the width of a representative tracheal tube throughout multiple compression cycles. Movie sequences were imported into NIH Image and landmark points were digitized using QuickImage software (Walker, 2001). For each specimen, a large tracheal tube (for most, a main tube of the mesothorax) was used. Because in general the amount of compression varied with location along the tube, a point of maximal compression was chosen for digitization. Two points were digitized per frame, one on each side of the tracheal wall, oriented orthogonally (representing a diameter). Because line thickness in phase-contrast images is artifactual (i.e. the width of a line is greater than the true anatomical width), the boundary of the tracheal tube was estimated as the midpoint of the line width. The diameter of the tracheal tube was calculated as the distance between these two points. Five compression sequences for each specimen were digitized, with the beginning and ending of each compression sequence determined by tracheal movement patterns observed in the movie records.

Statistics

To test differences among pre-beam, beam on and post-beam treatments, we used JMP software (SAS Institute, Cary, NC, USA) to perform repeated measures ANOVA. Percentage data were arcsine transformed prior to analysis. *Post-hoc* Tukey–Kramer honestly significant difference (HSD) tests were used to determine specific differences between means.

RESULTS

Tracheal compression dynamics

As shown in the x-ray video records, tracheal compressions occurred in every segment of the body, including head, thorax (prothorax, mesothorax and metathorax) and abdomen (Fig. 2). In addition, compressions were observed in the leg (femur) and mouthparts (mandibles). No compressions occurred in the antennae. As shown in Fig. 2, not all tracheal tubes in a given body segment were compressed. Furthermore, there was variable compressibility along the length of a tube; in some tubes, certain sections remained inflated.

Tracheal compression cycles occurred at an average frequency of $15.6 \pm 4.2 \text{ cycles min}^{-1}$. These cycles displayed four phases (Fig. 3): collapse, in which the tracheal tube diameter decreased rapidly; static compression, in which the tube was held compressed at a minimum volume; reinflation, in which the tracheal tube diameter rapidly increased to its resting width; and inter-compression, during which tracheal tubes were open at their maximal diameter. The duration of a complete cycle was $4.17 \pm 1.02 \text{ s}$, with tubes compressed for $1.75 \pm 0.26 \text{ s}$ and open for $2.43 \pm 0.87 \text{ s}$ ($N=404$ cycles, 10 specimens). Collapse ($0.20 \pm 0.02 \text{ s}$, $N=31$ cycles, eight specimens) and reinflation ($0.40 \pm 0.13 \text{ s}$) were relatively fast; static compression ($0.99 \pm 0.33 \text{ s}$) comprised the majority of the duration of compression. Tube width decreased maximally by $66 \pm 6\%$ ($N=31$ cycles, eight specimens; Fig. 3D) during compression.

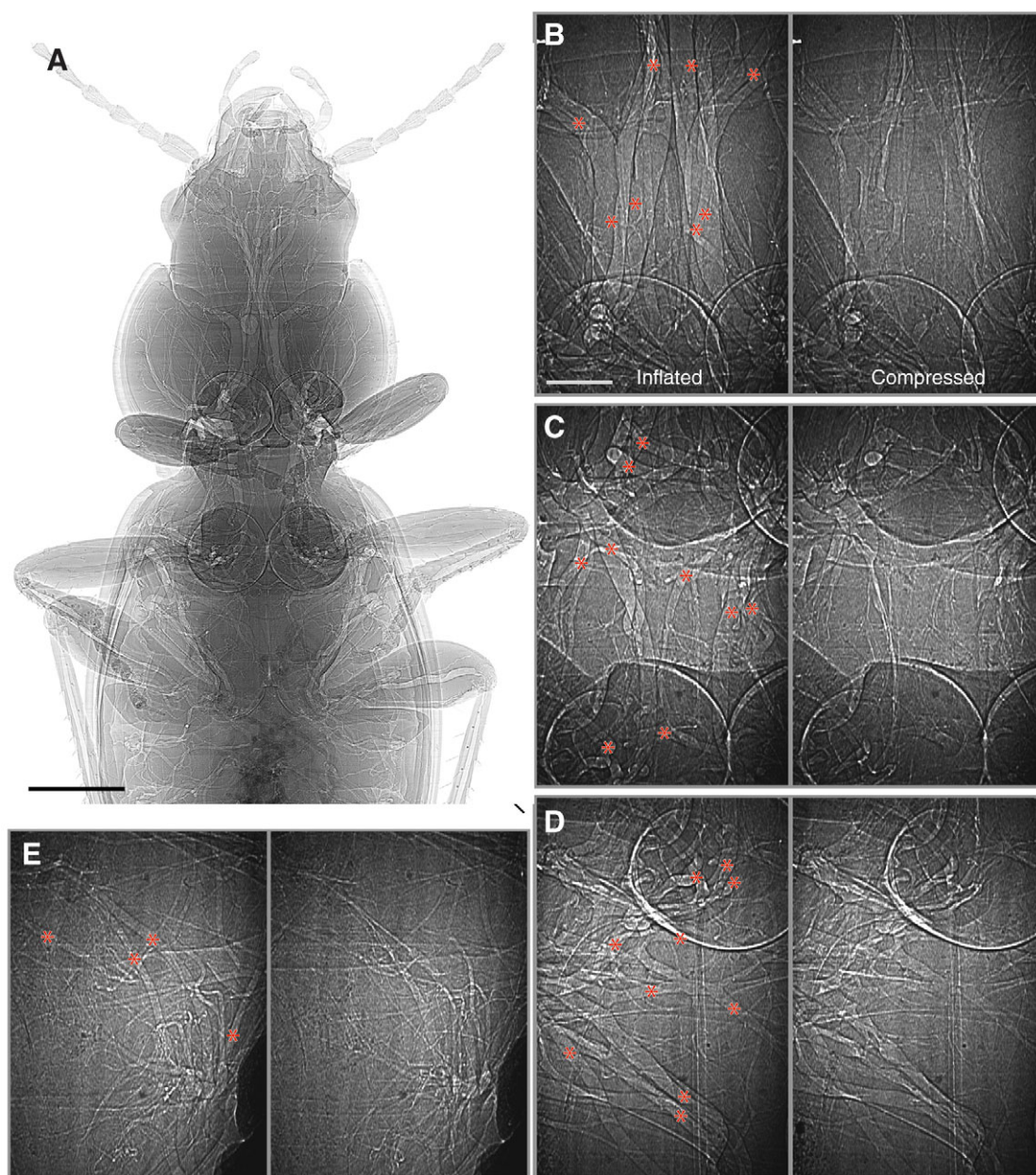


Fig. 2. Occurrence of rhythmic tracheal compression in different regions of the body of *Pterostichus stygicus*. (A) Tracheal system, showing tracheae in resting (inflated) posture. Image is a compilation of multiple x-ray images of a freshly killed specimen. Posterior abdomen not shown. (B–E) Movie stills showing inflated (left image) and compressed (right image) tracheae, depicting compression in the prothorax (B), mesothorax (C), metathorax (D) and posterior abdomen (E). Asterisks mark tracheal tubes that are compressed in the corresponding image. Compressions also occurred in the head and legs (not shown). Scale bars: 1 mm (A), 200 μ m (B–E).

Relationship between tracheal compression and external gas exchange

For each and every tracheal compression observed in the x-ray video, there was a corresponding local peak in the CO₂ trace; there were no compressions that occurred in the absence of a CO₂ peak (Figs 4 and 5). The lag between the start of compression and the rise in CO₂ was 0.16 ± 0.24 s in specimens synchronized with low precision ($N=7$), and 0.11 ± 0.04 s in specimens synchronized with higher precision ($N=2$). In the light of the synchronization error (± 0.97 and ± 0.07 s, respectively), we cannot distinguish these values as different from zero, but these data show that the start of tracheal compression and the start of CO₂ rise occurred almost simultaneously. In some

instances, the burst of CO₂ was followed immediately by a local decrease in CO₂ output (e.g. Fig. 4); however, other specimens did not show this pattern (e.g. Fig. 5).

To determine the contribution of tracheal compression to the total CO₂ output, we calculated the volume of gas in a subsample of the CO₂ bursts associated with compressions. In most specimens, these peaks appeared to be superimposed on a background level of CO₂ output. We calculated the volume of such pulses assuming baseline CO₂ values at the start and end of the pulse (Fig. 6A). These pulses contained 20 ± 9 nl of CO₂, were 2.5 ± 0.8 s in duration, and represented 20% of the average CO₂ emission (Table 1; $N=80$ pulses). In pre-beam traces, similar CO₂

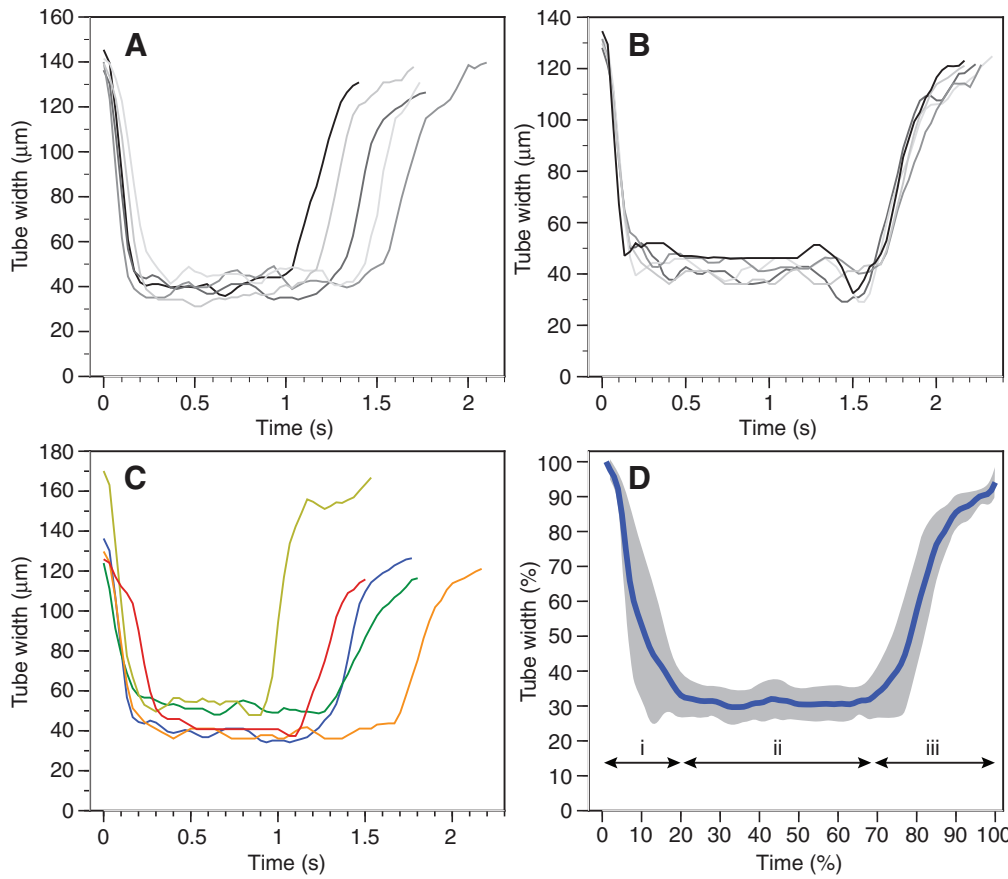


Fig. 3. Kinematics of tracheal compression in *Pterostichus stygicus*. Data depict width changes at one location (Fig. 1, blue arrow) of a primary tracheal tube located in the mesothorax. For comparison, the compression cycles are overlaid at time zero. (A,B) Variation in compression cycles within two individual beetles. In A, the beetle (mass 193.0 mg) used similar compression and re-inflation dynamics, but with variable duration of the compressed phase. The beetle in B (mass 155.7 mg) displayed highly regular compression cycles. (C) Average compression cycles for five individuals. Each line represents an average of five compression cycles for each individual. (D) Summary of compression dynamics: i, collapse; ii, static compression; iii, re-inflation. Blue line represents the average of the five individuals in C, each normalized to percentage width and percentage time. Gray shading represents 1 s.d. from the mean.

pulses (which we assume were produced *via* tracheal compression) accounted for 13% of the average emission.

We wondered whether we might be underestimating the contribution of tracheal compressions to CO₂ emission because the time resolution of our respirometry system was insufficient to discern the true drop in CO₂ emission that occurred between compressions.

If compressions occurred rapidly enough, the individual bursts may have been superimposed. To test this possibility, we took advantage of a single trial in which the beetle occasionally compressed its tracheae during periods of zero (or near-zero) background CO₂ release, providing isolated ‘singlet’ pulses (Fig. 6A). We used a large singlet burst (Fig. 6A, red arrow) to determine the effect of

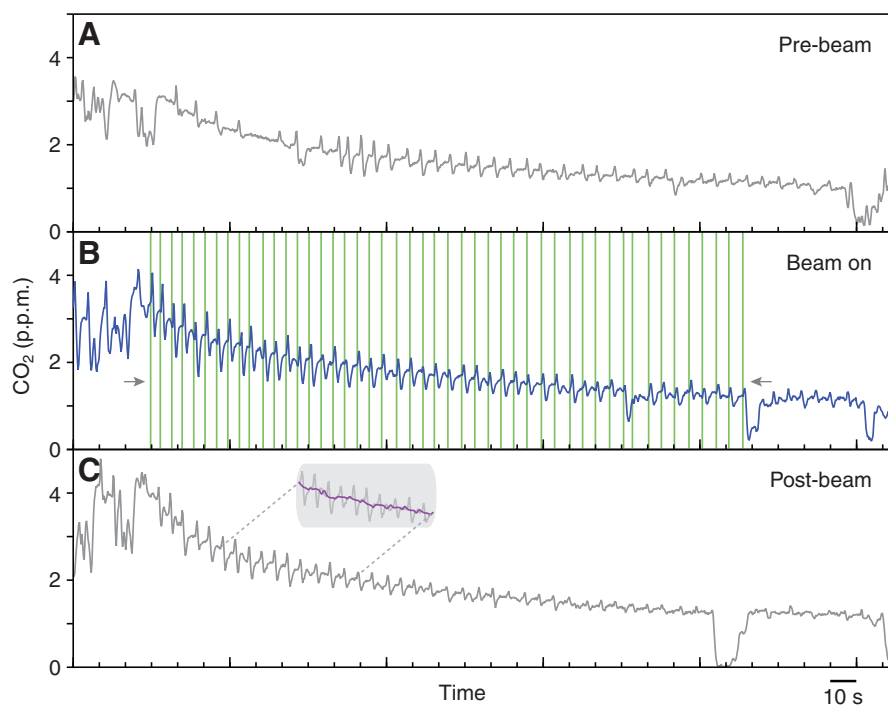


Fig. 4. Correlation of tracheal compressions with respiratory pulses of CO₂ in *Pterostichus stygicus*. Data are from one trial (mass 280.0 mg) showing representative CO₂ emission before x-ray exposure (A), during x-ray exposure (B), and after x-ray exposure (C). Green vertical lines indicate the start of a tracheal compression, identified from x-ray movie records (digitized block between pair of arrows, $t=3.8$ min). The inset box in C depicts a simulated CO₂ trace using a 1/10 slower flow speed: 150 ml min⁻¹ (purple) vs 1.5 l min⁻¹ (gray). To simulate the slower speed, CO₂ data were smoothed using a running average of 15 points (4.5 s); this interval was chosen to approximate the transit time of gas through the infrared detector at this flow speed (see Gray and Bradley, 2006). Simulated low flow speeds obscure the prominent high-frequency component of the signal.

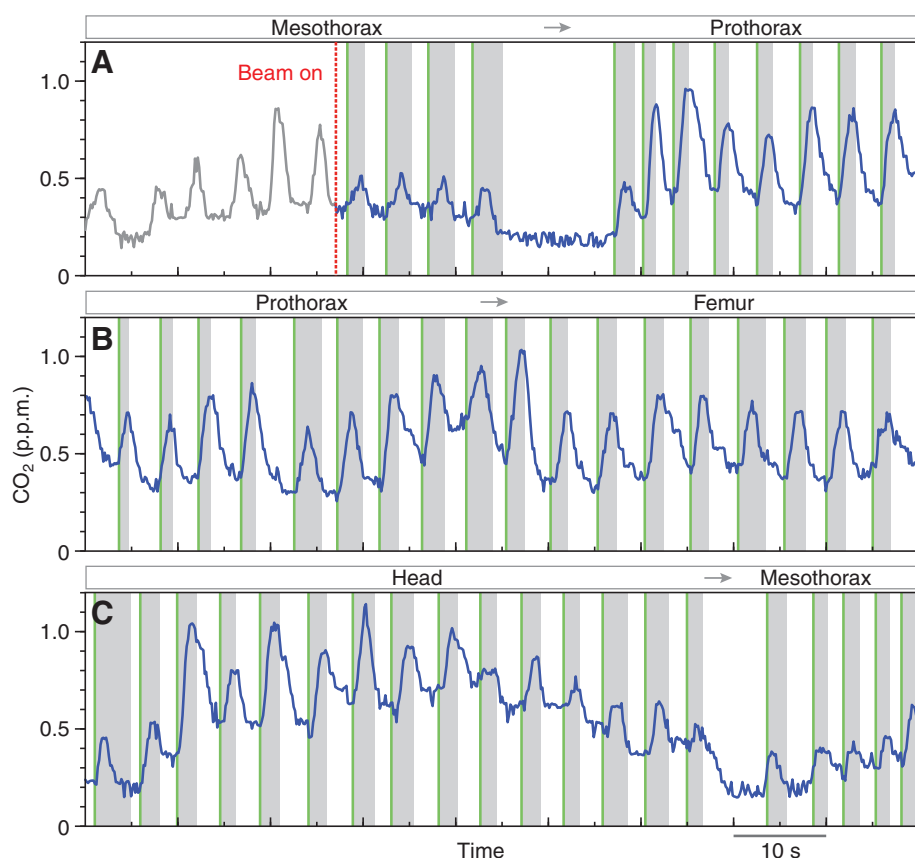


Fig. 5. Details of the relative timing of tracheal compressions and CO₂ pulses in different regions of the body of *Pterostichus stygicus*. Gray banding represents the total duration of the compression cycle (from collapse to reinflation), identified from movie records. The green lines indicate the start of compression, with line thickness representing the duration of tracheal collapse phase. The boxes above each trace indicate which part of the beetle was in (x-ray) view during CO₂ recording; arrows represent translation of the beetle to a different body region. Data are from one specimen (mass 130.0 mg).

superimposition by simulating burst repeat rates of 14, 20, 33 and 50 min⁻¹ (Fig. 6B). At the compression frequencies near those measured for the beetle, CO₂ emission rate dropped to near zero, and high continuous baselines of CO₂, as recorded in all beetles, did not occur until frequencies were much greater than those actually observed. This simulation suggests that our estimate of CO₂ emission associated with tracheal compressions was not significantly underestimated by the time resolution of our respiratory system. The baseline CO₂ emission is probably due to diffusive CO₂ emission through open spiracles, or is associated with convection occurring at frequencies higher than we could observe with our measuring system.

Effect of x-ray beam on gas exchange patterns

Although tracheal compressions could not be visualized without the x-ray beam on, similar pulses of CO₂ occurred both prior to and after the x-ray beam irradiation (Figs 4, 5 and 7). On average, these pulses were not significantly different in frequency (ANOVA: $F_{2,25}=1.90$, $P=0.17$) or duration (ANOVA: $F_{2,23}=1.75$, $P=0.20$) in pre-beam, beam on and post-beam treatments, and the average mass-specific metabolic rate did not vary (ANOVA: $F_{2,23}=0.45$, $P=0.64$; Table 1; Fig. 8). The only variable that changed was absolute CO₂ pulse volume, which was approximately twice as large when the x-ray beam was turned on (ANOVA: $F_{2,23}=4.26$, $P=0.03$; Tukey–Kramer HSD $P<0.05$); however, it was not significantly

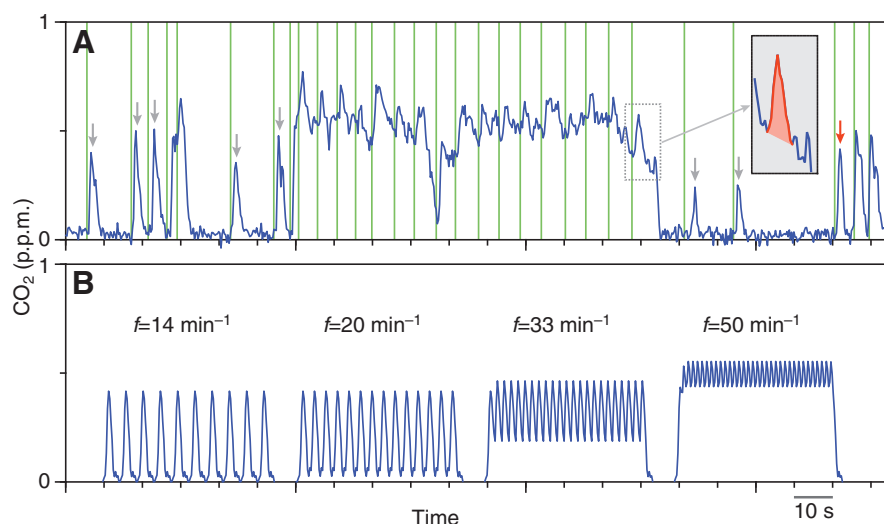


Fig. 6. (A) Occurrence of CO₂ pulses from zero and non-zero baseline CO₂ in one specimen of *Pterostichus stygicus*. 'Singlet' pulses (indicated with grey arrows) were stand-alone bursts of CO₂ that occurred with a tracheal compression. Such singlets did not occur in any other specimen. The inset box shows the area (red) used to calculate the volume of all other pulses. Beetle, mass 178.0 mg. (B) Multiple repeating CO₂ bursts used to simulate patterns of superimposition (without additional CO₂). A large singlet burst (red arrow in A) was repeated at frequencies (f) of 14, 20, 33 and 50 min⁻¹.

Table 1. Summary of pre-beam, beam on, and post-beam characteristics of gas exchange patterns

	Mean	Range	N
Pre-beam			
CO ₂ pulse frequency (min ⁻¹)	12.2±3.8	6.1–16.9	8
CO ₂ pulse duration (s)	2.0±0.4	1.3–2.4	8
CO ₂ pulse volume (nl)	8.3±6.6	2.1–21.8	8
Average CO ₂ in pulse/total CO ₂ emission (%)	12.9±11.5	1.9–29.0	6
Average metabolic rate (ml CO ₂ g ⁻¹ min ⁻¹)	0.0080±0.0041	0.0024–0.0153	8
Beam on			
CO ₂ pulse frequency (min ⁻¹)	15.6±4.2	10.9–26.2	10
CO ₂ pulse duration (s)	2.5±0.8	1.5–3.4	8
CO ₂ pulse volume (nl)	19.8±9.1*	12.1–34.5	8
Average CO ₂ in pulse/total CO ₂ emission (%)	20.3±11.7	8.0–40.1	8
Average metabolic rate (ml CO ₂ g ⁻¹ min ⁻¹)	0.0106±0.0051	0.0044–0.0187	8
Post-beam			
CO ₂ pulse frequency (min ⁻¹)	13.6±3.0	8.4–18.1	8
CO ₂ pulse duration (s)	2.0±0.6	1.1–2.7	8
CO ₂ pulse volume (nl)	10.4±9.0	3.9–30.6	8
Average CO ₂ in pulse/total CO ₂ emission (%)	11.0±10.3	2.2–29.9	7
Average metabolic rate (ml CO ₂ g ⁻¹ min ⁻¹)	0.0096±0.0068	0.0030–0.0240	8

Volume and duration of peaks refer to CO₂ bursts correlated with tracheal compressions. Amongst treatments, only CO₂ pulse volume was significantly different, as indicated with an asterisk.

different (ANOVA: $F_{2,20}=1.73$, $P=0.21$) when calculated as a fraction of the total CO₂ released. When considering individual trials, most specimens changed some aspect of their gas exchange pattern during irradiation (e.g. Fig. 7), including increased tracheal compression frequency (5 of 8 specimens) and increased volume per pulse (6 of 8 specimens). These changes suggest that exposure to the x-ray increased the magnitude of tracheal compression. However, the fact that similar patterns of CO₂ pulses occurred in and out of the x-ray beam strongly suggests that tracheal compression occurs in inactive beetles. Interestingly, in one trial the beetle stopped compressing when the beam was turned on (see supplementary material Fig. S1), and resumed compressing after the beam was turned off, suggesting that occasionally these beetles may silence their tracheal compressions in response to disturbance or stress.

DISCUSSION

Tracheal compressions are associated with external gas exchange in the carabid beetle *Pterostichus stygicus*. Each compression occurred on a one-to-one basis with a burst of expelled CO₂, representing approximately 13% of gas exchange in non-irradiated animals. The bulk of our CO₂ records show that tracheal compressions occurred during a continuous background release of CO₂, indicating that at least one spiracle was open in-between compressions. Given that the start of a compression occurred

virtually simultaneously with the local rise in CO₂ release, we conclude that compressions functioned to convectively push air across the spiracles and out of the beetle's body. This is the first study to causally link the dynamics of deformable tracheae to specific external gas exchange patterns with high temporal resolution.

Stress of the x-ray environment

Given sufficient time, synchrotron x-rays used to image the tracheal system will change the respiratory pattern and kill most insects (Socha et al., 2007). Are the tracheal compressions reported here a consequence of the stress of x-ray imaging, or do they also occur in unirradiated animals? The observation that respiratory patterns are very similar in pattern and frequency of bursts before and during initial beam exposure strongly suggests that tracheal compressions were occurring in the beetles prior to x-ray exposure. These beetles were clearly not 'undisturbed', as they had been handled in the hour prior to recording, and their movements were constrained. Thus we cannot say for certain whether tracheal compressions occur in beetles under other conditions, for example when foraging in the field, or when kept in the dark without food for many hours, as is sometimes done with insects to record discontinuous gas exchange. However, it does not appear that these beetles were under excessive stress, as their metabolic rates [average: 0.0090 ml CO₂ g⁻¹ min⁻¹, 95% confidence interval (CI):

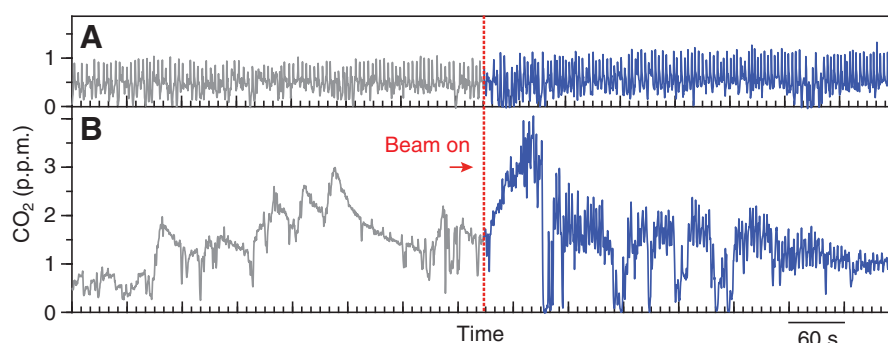


Fig. 7. Effect of x-ray beam on CO₂ release in *Pterostichus stygicus*. Traces from two specimens are shown, depicting extremes of the response to irradiation. The beetle (mass 219.5 mg) in A shows no change in average CO₂ pulse frequency (15.7 min⁻¹) or volume (0.013 µl), whereas the beetle (mass 166.3 mg) in B shows an increase in both frequency (8.1 to 16.2 min⁻¹) and volume (0.004 to 0.024 µl).

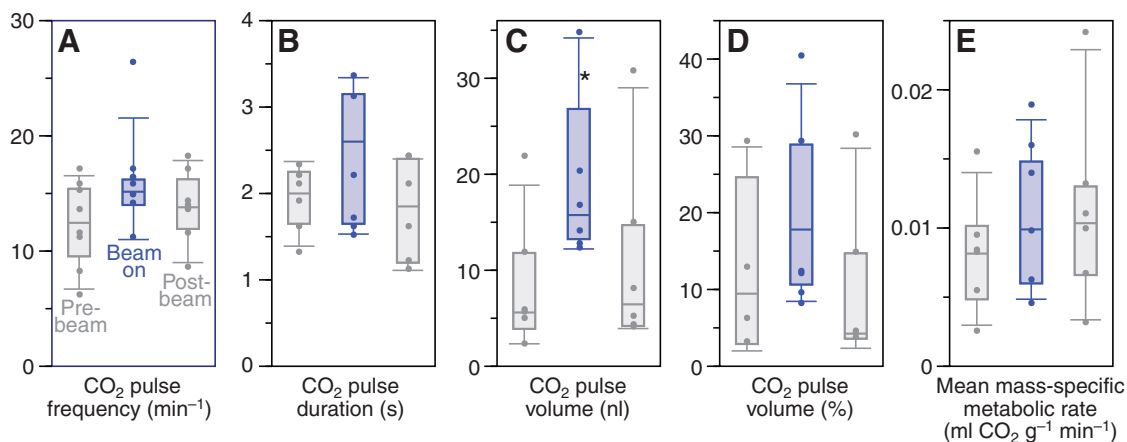


Fig. 8. Comparison of gas exchange patterns during pre-beam, beam on and post-beam treatments. Only CO₂ pulse volume (C) showed significant differences (asterisk); beam on volumes were greater than those of both pre- and post-beam. The top, bottom and line through the middle of the box correspond to the 75th, 25th and 50th percentile (median), respectively; whiskers extend from the 10th and 90th percentiles.

0.0060–0.0121 ml CO₂ g⁻¹ min⁻¹, $N=9$] overlapped the predicted value for resting carabid beetles reported by Chown and colleagues [predicted value for a 181 mg beetle, with respiratory quotient RQ=0.85: 0.0067 ml CO₂ g⁻¹ min⁻¹ (Chown et al., 2007)]. Thus, tracheal compressions occurred in beetles exhibiting metabolic rates in the range of those considered ‘resting’ by the current literature. Exposure to the beam did double the amount of CO₂ emitted per pulse, suggesting that variation in tracheal compression may be an important mechanism of grading gas exchange in response to stress or metabolic need.

The role of convection in *Pterostichus stygicus*

Generally, in species that deform parts of the tracheal system, patterns of CO₂ release should depend on the kinematics of compression, the connectivity of the tracheal system, and the timing of spiracle opening and closing. In *Pterostichus stygicus*, the exact architecture of the tracheal system and the spiracle dynamics are not yet known, but because at least one spiracle was open at the start of a compression, the air displaced during tracheal deformation must have contributed to a convective movement of air out of the body.

How does the volume of compressed tracheae compare with the volume of expressed air? To explore this question, we estimate the volume of air displaced in the tracheae and compare it with the volume of air in the recorded CO₂ bursts. As a simple first-order model, we consider only the major tracheal tubes involved in compression and assume round, cylindrical tubes with dimensions based on the measured anatomy of a typical specimen of *Pterostichus stygicus* (Fig. 9; mass=182 mg). In this model, the resting (uncompressed) volume of the trachea section is 468 nl. To calculate the volume of air displaced in the tubes during compression, we follow Westneat and colleagues (Westneat et al., 2003) and assume a uniform cross-sectional shape change in the tracheae from circular to elliptical and a constant perimeter. In this model, a tracheal tube width change of 60–72% would displace 197–272 nl of air. Assuming CO₂ partial pressures in the tracheae of 1–5%, the CO₂ volume is therefore calculated to be 2–14 nl. This estimated displaced gas in the tracheae overlaps the measured range of CO₂ burst volumes (4–40 nl). Although we have made many simplifying assumptions, this comparison lends plausibility to our conclusion that tracheal compressions convectively pushed air out

of the beetle’s body. Precise calculations of displaced volume require a more thorough understanding of the location and three-dimensional geometry of compression, or experimental manipulations to controllably produce collapse. We are currently conducting detailed morphological analyses to precisely determine the volume of air displaced during compression; in theory these measurements can be combined with CO₂ emission rates to estimate the percentage CO₂ in the expired air.

Theoretically, it remains possible that the CO₂ bursts we observed were purely diffusive in origin, and not actually linked to tracheal compressions. Diffusive bursts simultaneous with tracheal compressions could occur if the compressed tubes were located

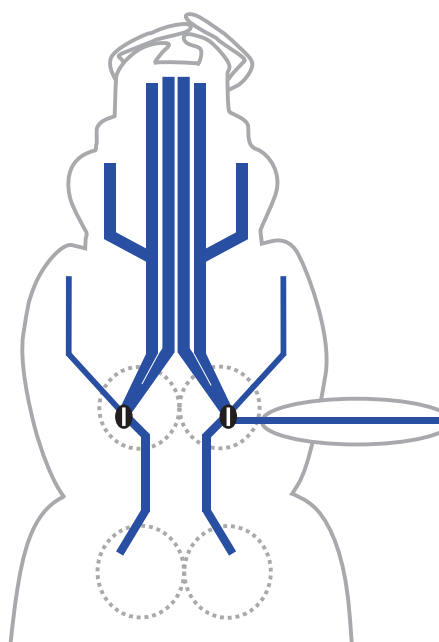


Fig. 9. Model of the tracheal system used to estimate the volume of displaced air during a tracheal compression in *Pterostichus stygicus*. Black ovals depict the thoracic spiracles. The main trachea of each femur was used (six total); only one is depicted for clarity.

exclusively in a sealed part of the insect, with spiracles closed; CO₂ bursts then might originate from an uncompressed part of the tracheal system by the opening of separate spiracles. Under these conditions, tracheal compressions would act on an enclosed volume of air, pressurizing the internal air, or expanding another part of the system. Two lines of evidence argue against this scenario. First, no section of tracheae appeared to increase in volume during compression of the system. Second, aside from a few basal groups, most insects are understood to have continuous, non-compartmentalized tracheal systems (e.g. Hetz, 2007; Wigglesworth, 1931), and our high-resolution x-ray images have not revealed any evidence of valving or compartmentation in the tracheal system of *Pterostichus stygicus*. Direct confirmation that tracheal compression drives air through the spiracles will require measurement of airflow through the spiracles, or the contributions of convection and diffusion could be quantified by manipulating the density of the air in the flow-through system by replacing N₂ with SF₆ or helium.

Observations of collapsible tracheae in insects

It has long been recognized that insect tracheal structures (including both tracheal tubes and air sacs) are capable of being compressed. In fact as far back as 1931, Wigglesworth noted that it was generally accepted that respiratory movements such as abdominal and thoracic pumping function to alternately compress and dilate the tracheal system (Wigglesworth, 1931). However, the mechanical problem with this idea is that taenial rings, which are thickenings in the tracheal wall, can be viewed as morphological specializations that prevent rather than promote collapse. Given the ubiquity of taenidia in insect tracheae, the current prevailing view is that most tracheae act as rigid conduits rather than flexible bellows-like structures. Collapse, then, is seen as an exception, occurring only in places with reduced taenidia, thinner walls or non-circular tubes. Of the latter, Krogh used the term 'respiration tracheae' or 'ventilation tracheae' to describe special distensible tracheae that feature an oval rather than a round cross-sectional shape (Krogh, 1920b; Krogh, 1941); such tracheae were implicated by Miller to be involved in convective airflow in large, flying, cerambycid beetles (Miller, 1966b). However, these ideas of compressibility rely largely on anatomical inference (e.g. Kerry and Mill, 1987; Komai, 1998), and very few studies have described compressions in living animals, largely due to methodological limitations.

Because so few direct *in vivo* observations of collapsible tracheae have been made, it is difficult to assess in what ways the rhythmic tracheal compression seen here and in other species relates to known gas exchange mechanisms. Prior to synchrotron imaging, the only way to directly view activity in the tracheal system was in translucent animals using visible light. Dunavan observed what appear to be similar compression cycles in fly larvae (*Erstalis arbustorum*) after starving them of oxygen (Dunavan, 1929). Upon reintroduction to air, the larvae were seen (*via* microscope) to rapidly 'flatten' and then to reinflate the two main tracheal trunks, with about 2 s between cycles. Compression events were not quantified, precluding comparison of duration or frequency. However, reinflation was described as taking place more slowly than collapse, perhaps similar to that in *Pterostichus stygicus*, in which reinflation was about twice as slow as compression. In another example, Herford viewed what was termed 'tracheal pulsation' in the thorax, abdomen and legs of several species of flea (Herford, 1938). In a tracheal pulsation, the main tracheal tubes were seen to collapse slowly over the course of about 30 s, and then rapidly reinflate, with 5–80 s between compressions; the tubes straightened along their length during collapse as well. In contrast to the so-called 'ventilation tracheae'

of Krogh, these tracheae were round in resting cross-section, not oval. Additionally, the pulsations ceased entirely when the legs were cut open, such that the tracheae became permanently connected to the atmosphere. In both the fly larvae and the fleas, it is not understood what produced the compression cycles, but the mechanism is probably quite different between *Pterostichus stygicus* (and fly larvae) and fleas. Their slow tracheal collapse, rapid reinflation and cessation of cycles with opening to the environment point to passive suction ventilation (PSV) as the mechanism (Buck, 1962). If true, the fleas' tracheae collapsed as oxygen was depleted in a sealed system (with spiracles closed), and reinflated rapidly when spiracles opened. These tracheal dynamics are the inverse of those in the larvae and beetles, which showed rapid collapse and slower reinflation. Indeed, we reject the hypothesis that PSV produced tracheal compressions in *Pterostichus stygicus* because CO₂ traces indicated that spiracles were open at the start of most compressions.

Tracheal compressions in *Pterostichus stygicus* were similar in nature to those described in the carabid beetle *Platynus decentis* (Westneat et al., 2003), but differences in compression characteristics are evident. In contrast to *Pterostichus stygicus*, compressions in *Platynus decentis* were dynamically symmetrical, with collapse and reinflation taking place at the same rate; also, there was no static compression phase in which the tubes were held deflated in place. Compressions in *Platynus decentis* were shorter in duration (0.7 vs 1.8 s) and occurred more frequently (42 vs 16 min⁻¹). These differences may be related to body size, metabolism or other physiological factors. Alternatively (or in addition), they may reflect differences in x-ray effects on the animals: improvements in our imaging system have resulted in the ability to use a lower beam intensity to achieve the same or higher quality imagery than used previously (Socha et al., 2007), and *Platynus decentis* may have been under greater irradiative duress than *Pterostichus stygicus*.

Anatomical mechanism of tracheal compression

Two general mechanisms may have produced rhythmic tracheal compressions in *Pterostichus stygicus*. The first is collapse by direct mechanical impingement of the tube; this deformation could hypothetically be effected by the muscle width increase that occurs during normal isovolumetric shortening (Kier and Smith, 1985; Komai, 1998). However, this hypothesis seems unlikely given the synchronous collapse of tracheal tubes throughout the body and the fact that insect tracheae are amuscular (Whitten, 1972). The second possible mechanism is collapse by differential pressure across the tracheal wall. This pressure difference could arise from decreased intra-tracheal pressure, increased hemolymph pressure or some combination of both. Miller (1966b) experimentally determined that large secondary tracheae (diameter ~300 μm) excised from the cerambycid beetle *Petrognatha gigas* collapsed under a pressure difference of 0.7–2.4 kPa. Comparable hemolymph pressure changes have been recorded in the hemocoel of live animals, including 0.5 kPa in lepidopteran and coleopteran pupae (e.g. Sláma, 2000; Sláma and Neven, 2001) and 1–2 kPa in adult desert locusts (Krolkowski and Harrison, 1996; Weis-Fogh, 1967), suggesting that hemolymph pressure changes are capable of producing the observed tracheal compressions in *Pterostichus stygicus*. Given the synchronicity of collapse, we suggest that global pressure change is the primary mechanism of tracheal compression in *Pterostichus stygicus* and other carabid beetles that display this behavior. However, a puzzling question remains: if hemolymph pressure is the cause, why do some tracheal tubes not collapse? One possibility is that variation in tracheal tube mechanical properties underlies differences in local tube compressibility.

Cyclic changes in coelomic hemolymph pressure with frequencies similar to the tracheal compressions observed here have been recorded in multiple species (Coquillaud et al., 1990; Sláma, 1989; Sláma, 2000; Sláma, 1984; Sláma and Neven, 2001). Sláma has termed these coelomic pulsations ‘extracardiac’ to distinguish them from those produced by contractions of the dorsal heart vessel, which give rise to pressure changes roughly two orders of magnitude smaller (Sláma, 2000). Extracardiac hemolymph pulsations have been associated with external gas exchange and have been suggested to play a major role in insect respiration (Sláma, 1999). Further studies will be required to determine whether the CO₂ and pressure pulsations documented by Sláma and colleagues are identical to the tracheal compression-linked CO₂ pulsed in *Pterostichus stygicus*. However, the patterns are so similar that this seems quite likely, further supporting the hypothesis that tracheal compression is a mechanism for enhancing trans-spiracular gas exchange in many insects. If so, the system may work mechanically *via* the following sequence, hypothesized by Sláma (Sláma, 1994): (1) muscular contraction of abdominal segments; (2) decrease in body volume; (3) increase in pressure and movement of hemolymph in the hemocoel; and (4) compression of the main tracheal trunks, resulting in mechanical (convective) expulsion of intratracheal gas through the open spiracles. Our study provides positive evidence for the last component (compression of tubes and expulsion of gas), but we have yet to test the other aspects of this model. To this end, we are currently exploring the relationship between external body movements, internal pressure changes, tracheal collapse and gas exchange in *Pterostichus stygicus* and other species.

Physiological function of tracheal compression

Are the tracheal compressions observed here necessary for adequate gas exchange in beetles and other insects? Classic respiration studies (Krogh, 1920a; Weis-Fogh, 1964) have shown that diffusion alone should deliver sufficient oxygen to support resting metabolic rate in insects. Is it possible for diffusion to suffice to deliver oxygen from the mesothoracic spiracles to the head *via* the four main tracheal trunks? We consider the simplest case: we model the four tracheae as one conduit with summed area, the head alone consumes oxygen (i.e. there is no metabolic loss of oxygen along the length of the tube), and spiracles are open to atmospheric oxygen. The rate of oxygen delivery to the head (m/t) is then given by Fick’s equation:

$$\frac{m}{t} = DA \frac{C}{L}, \quad (2)$$

where D is the diffusion coefficient, A is the cross-sectional area of the tracheal tube, C is the concentration difference and L is the length of tube. In this estimate, we consider a tube with a 400 μm radius and length of 4 mm, values that reflect the four primary tracheae that lead to the head in *Pterostichus stygicus*. Using a value of 0.219 cm² s⁻¹ for the diffusion coefficient of oxygen at 20°C, the oxygen delivery rate to the head is 0.035 ml min⁻¹. For the consumption rate of the head, we use the average pre-beam mass-specific metabolic rate (0.01 l ml O₂ g⁻¹ min⁻¹) and estimate the head mass to be 20% of total body mass; this gives a consumption rate of 0.0004 ml O₂ min⁻¹. Thus the estimated oxygen consumption rate of the head is almost an order of magnitude smaller than the potential delivery rate by diffusion alone, suggesting that convection is not strictly necessary for oxygen delivery in the resting beetle. The high baseline CO₂ emission in the absence of observable tracheal

compressions provides further direct evidence of a significant role for diffusion in the gas exchange of this beetle.

If diffusion can sustain adequate gas exchange, why do tracheal compressions occur? One possibility is that the increase in gas exchange associated with the tracheal compressions functions to keep oxygen partial pressures high at the tissues for sudden fast movement; in grasshoppers, a significant portion of the oxygen consumed during seconds of jumping comes from internal tracheal stores (Harrison et al., 1991). Convection may promote equalization of oxygen and carbon dioxide levels throughout the insect, aiding metabolic and acid–base regulation. Another possibility, as argued by Kestler (Kestler, 1985), is that small insects may employ convective gas exchange where diffusion alone would be sufficient in order to minimize water loss through the spiracles.

Conclusion

This study illustrates the power of visualizing the internal dynamics of living insects. We would not have looked for high-frequency CO₂ bursts in *Pterostichus stygicus* without the discovery of rhythmic compressions in related taxa. Historically, most studies of gas exchange in insects that use flow-through respirometry have employed low flow speeds, which are well suited for determining broad-scale exchange patterns with high concentration precision, but, with poor temporal resolution, are ill-suited for characterizing short-duration events (see Fig. 4C) (Gray and Bradley, 2006). We suggest that some, if not many, of these previously studied taxa may show evidence of cyclic convective gas exchange when studied with higher flow speeds and when tracheal dynamics are revealed with synchrotron x-rays. Species that have been shown to use body movements or other high-frequency ventilatory signatures (e.g. Kuusik et al., 2001; Miller, 1971; Tartes et al., 1999) are particularly favorable for investigation. For example, the recently discovered correlation of cyclic gas exchange with proboscis extension movements in *Drosophila* (Lehmann and Heymann, 2005) may be mechanically explained by expansion of air sacs in the head, which can be readily visualized with x-rays (Westneat et al., 2008). Bursts of convectively expelled CO₂ *via* tracheal compression can occur during the F- and O- phases of discontinuous gas exchange cycles (Chown et al., 2006; Lighton, 1991; Lighton, 1996), and these may be associated with tracheal compressions. Considering the large diversity of recognized external gas exchange patterns in insects (Marais et al., 2005), it seems likely that internal compressions are used in ways other than that seen here in *Pterostichus stygicus* amongst the tremendous diversity of unexplored taxa.

We thank Melina Hale for use of the Picospritzer III, John Lighton and Jaco Klok for discussion, Alexander Kaiser for critical reading of the manuscript, Steve Deban for advice, and Kendra Greenlee for providing suggestive preliminary data on respirometry for *Platynus decentis*. We also thank two anonymous reviewers for helpful comments. Use of the Advanced Photon Source was supported by the US Department of Energy, Office of Science, Office of Basic Energy Sciences, under Contract No. DE-AC02-06CH11357.

REFERENCES

- Amos, W. B. and Miller, P. L. (1966). The supply of oxygen to the active flight muscles of *Petrognatha gigas* (F.) (Cerambycidae). *Entomologist* **98**, 88–94.
- Babak, E. (1921). Die Mechanik und Innervation der Atmung. In *Handbuch der Vergleichenden Physiologie*. Vol. 1 (ed. H. Winterstein), pp. 265–640. Germany: Gustav Fischer.
- Bartholomew, G. A. and Barnhart, M. C. (1984). Tracheal gases, respiratory gas exchange, body temperature and flight in some tropical cicadas. *J. Exp. Biol.* **111**, 131–144.
- Bartholomew, G. A., Vleck, D. and Vleck, C. M. (1981). Instantaneous measurements of oxygen consumption during pre-flight warm-up and post-flight cooling in sphingid and saturniid moths. *J. Exp. Biol.* **90**, 17–32.

- Buck, J.** (1962). Some physical aspects of insect respiration. *Annu. Rev. Entomol.* **7**, 27-56.
- Chapman, R. F.** (1998). *The Insects: Structure and Function*. Cambridge: Cambridge University Press.
- Chown, S. L., Gibbs, A. G., Hetz, S. K., Klok, C. J., Lighton, J. R. and Marais, E.** (2006). Discontinuous gas exchange in insects: a clarification of hypotheses and approaches. *Physiol. Biochem. Zool.* **79**, 333-343.
- Chown, S. L., Marais, E., Terblanche, J. S., Klok, C. J., Lighton, J. R. B. and Blackburn, T. M.** (2007). Scaling of insect metabolic rate is inconsistent with the nutrient supply network model. *Funct. Ecol.* **21**, 282-290.
- Coquillaud, M. S., Sláma, K. and Labeyrie, V.** (1990). Regulation of autonomic physiological functions during reproductive diapause of *Bruchus affinis*. In *Bruchids and Legumes: Economics, Ecology and Coevolution* (ed. K. Fujii, A. M. R. Gatehouse, C. D. Johnson, R. Mitchel and T. Yoshida), pp. 37-44. Netherlands: Kluwer Academic Publishers.
- Dudley, R.** (2000). *The Biomechanics of Insect Flight*. Princeton, NJ: Princeton University Press.
- Dunavan, D.** (1929). A study of respiration and respiratory organs of the rat-tailed maggot, *Erstalis arbustorum* L. (Diptera: Syrphidae). *Ann. Entomol. Soc. Am.* **22**, 731-753.
- Fitzgerald, R.** (2000). Phase-sensitive x-ray imaging. *Phys. Today* **53**, 23-26.
- Gray, E. M. and Bradley, T. J.** (2006). Evidence from mosquitoes suggests that cyclic gas exchange and discontinuous gas exchange are two manifestations of a single respiratory pattern. *J. Exp. Biol.* **209**, 1603-1611.
- Harrison, J. F.** (1997). Ventilatory mechanism and control in grasshoppers. *Am. Zool.* **37**, 73-81.
- Harrison, J. F., Phillips, J. E. and Gleeson, T. T.** (1991). Activity physiology of the two-striped grasshopper, *Melanoplus bivittatus*-gas-exchange, hemolymph acid-base status, lactate production, and the effect of temperature. *Physiol. Zool.* **64**, 451-472.
- Herford, G. M.** (1938). Tracheal pulsation in the flea. *J. Exp. Biol.* **15**, 327-338.
- Hetz, S. K.** (2007). The role of the spiracles in gas exchange during development of *Samia cynthia* (Lepidoptera, Saturniidae). *Comp. Biochem. Physiol., Part A Mol. Integr. Physiol.* **148**, 743-754.
- Kerry, C. J. and Mill, P. J.** (1987). An anatomical study of the abdominal muscular, nervous and respiratory systems of the praying mantid, *Hierodula membranacea* (Burmeister). *Proc. R. Soc. Lond., B, Biol. Sci.* **229**, 415-438.
- Kestler, P.** (1985). Respiration and respiratory water loss. In *Environmental Physiology and Biochemistry of Insects* (ed. K. H. Hoffman), pp. 137-183. Berlin: Springer.
- Kier, W. M. and Smith, K. K.** (1985). Tongues, tentacles and trunks: the biomechanics of movement in muscular-hydrostats. *Zool. J. Linn. Soc.* **83**, 307-324.
- Komai, Y.** (1998). Augmented respiration in a flying insect. *J. Exp. Biol.* **201**, 2359-2366.
- Krogh, A.** (1920a). Studien über Tracheenrespiration. II. Über Gasdiffusion in den Tracheen. *Pflügers Arch. Gesamte Physiol. Menschen Tiere* **179**, 95-112.
- Krogh, A.** (1920b). Studien über Tracheenrespiration. III. Die Kombination von mechanischer Ventilation mit Gasdiffusion nach Versuchen an Dytiscuslarven. *Pflügers Arch. Gesamte Physiol. Menschen Tiere* **179**, 113-120.
- Krogh, A.** (1941). *The Comparative Physiology of Respiratory Mechanisms*. Philadelphia, PA: University of Pennsylvania Press.
- Krolukowski, K. and Harrison, J.** (1996). Haemolymph acid-base status, tracheal gas levels and the control of post-exercise ventilation rate in grasshoppers. *J. Exp. Biol.* **199**, 391-399.
- Kuusik, A., Tartes, U., Vanatoa, A., Hiiesaar, K. I. and Metspalu, L.** (2001). Body movements and their role as triggers of heartbeats in pupae of the Colorado potato beetle *Leptinotarsa decemlineata*. *Physiol. Entomol.* **26**, 158-164.
- Lehmann, F.-O. and Heymann, N.** (2005). Unconventional mechanisms control cyclic respiratory gas release in flying *Drosophila*. *J. Exp. Biol.* **208**, 3645-3654.
- Lighton, J. R. B.** (1991). Ventilation in Namib Desert tenebrionid beetles-mass scaling and evidence of a novel quantized flutter-phase. *J. Exp. Biol.* **159**, 249-268.
- Lighton, J. R. B.** (1996). Discontinuous gas exchange in insects. *Annu. Rev. Entomol.* **41**, 309-324.
- Mand, M., Kuusik, A., Martin, A. J., Williams, I. H., Luik, A., Karise, R., Metspalu, L. and Hiiesaar, K.** (2005). Discontinuous gas exchange cycles and active ventilation in pupae of the bumblebee *Bombus terrestris*. *Apidologie* **36**, 561-570.
- Marais, E., Klok, C. J., Terblanche, J. S. and Chown, S. L.** (2005). Insect gas exchange patterns: a phylogenetic perspective. *J. Exp. Biol.* **208**, 4495-4507.
- Miller, P. L.** (1966a). The regulation of breathing in insects. In *Advances in Insect Physiology*. Vol. 3, (ed. J. W. L. Beament, J. E. Treherne and V. B. Wigglesworth), pp. 279-354. New York: Academic Press.
- Miller, P. L.** (1966b). The supply of oxygen to the active flight muscles of some large beetles. *J. Exp. Biol.* **45**, 285-304.
- Miller, P. L.** (1971). Rhythmic activity in the insect nervous system: thoracic ventilation in non-flying beetles. *J. Insect Physiol.* **17**, 395-405.
- Miller, P. L.** (1974). Respiration: aerial gas transport. In *The Physiology of Insects*. Vol. 4 (ed. M. Rockstein), pp. 345-402. New York: Academic Press.
- Nugent, K. A., Paganin, D. and Gureyev, T. E.** (2001). A phase odyssey. *Phys. Today* **54**, 27-32.
- Schneiderman, H. A.** (1960). Discontinuous respiration in insects: role of the spiracles. *Biol. Bull.* **119**, 494-528.
- Sláma, K.** (1984). Recording of haemolymph pressure pulsations from the insect body surface. *J. Comp. Physiol., B, Biochem. Syst. Environ. Physiol.* **154**, 635-643.
- Sláma, K.** (1988). A new look at insect respiration. *Biol. Bull.* **175**, 289-300.
- Sláma, K.** (1989). Role of the autonomic nervous system (coelopulse) in insect reproduction. In *Regulation of Insect Reproduction*. Vol. 4, pp. 23-38. Zinkovy, Czechoslovakia: Academia.
- Sláma, K.** (1994). Regulation of respiratory acidemia by the autonomic nervous system (coelopulse) in insects and ticks. *Physiol. Zool.* **67**, 163-174.
- Sláma, K.** (1999). Active regulation of insect respiration. *Ann. Entomol. Soc. Am.* **92**, 916-929.
- Sláma, K.** (2000). Extracardiac versus cardiac haemocoelic pulsations in pupae of the mealworm (*Tenebrio molitor* L.). *J. Insect Physiol.* **46**, 977-992.
- Sláma, K. and Neven, L.** (2001). Active regulation of respiration and circulation in pupae of the codling moth (*Cydia pomonella*). *J. Insect Physiol.* **47**, 1321-1336.
- Socha, J. J., Westneat, M. W., Harrison, J. F., Waters, J. S. and Lee, W. K.** (2007). Real-time phase-contrast x-ray imaging: a new technique for the study of animal form and function. *BMC Biol.* **5**, 6.
- Stride, G. O.** (1958). The application of the Bernoulli equation to problems of insect respiration. *10th Int. Congr. Ent.* **2**, 335-336.
- Tartes, U., Kuusik, A. and Vanatoa, A.** (1999). Diversity in gas exchange and muscular activity patterns in insects studied by a respirometer-actograph. *Physiol. Entomol.* **24**, 150-157.
- Walker, J. A.** (2001). QuickImage: a modification of NIH Image with enhanced digitizing tools. <http://www.usm.maine.edu/~walker/software.html>
- Wasserthal, L. T.** (1996). Interaction of circulation and tracheal ventilation in holometabolous insects. In *Advances in Insect Physiology*. Vol. 26 (ed. P. D. Evans), pp. 297-351. London: Academic Press.
- Weis-Fogh, T.** (1964). Diffusion in insect wing muscle, the most active tissue known. *J. Exp. Biol.* **41**, 229-256.
- Weis-Fogh, T.** (1967). Respiration and tracheal ventilation in locusts and other flying insects. *J. Exp. Biol.* **47**, 561-587.
- Westneat, M. W., Betz, O., Blob, R. W., Fezzaa, K., Cooper, W. J. and Lee, W. K.** (2003). Tracheal respiration in insects visualized with synchrotron X-ray imaging. *Science* **299**, 558-560.
- Westneat, M. W., Socha, J. J. and Lee, W. K.** (2008). Advances in biological structure, function, and physiology using synchrotron x-ray imaging. *Annu. Rev. Physiol.* **70**, 119-142.
- Whitten, J. M.** (1972). Comparative anatomy of the tracheal system. *Annu. Rev. Entomol.* **17**, 373-402.
- Wigglesworth, V. B.** (1931). The respiration of insects. *Biol. Rev.* **6**, 181-220.